Electronic Supplementary Material (ESI) for ChemComm.

Supporting Information

Supramolecular chirality: A caveat in assigning the handedness of chiral aggregate

K. Swathi,[a,b] *Cristina Sissa,*[a] *Anna Painelli,*[a] *and K. George Thomas*[b]

[a]Dip. di Scienze Chimiche, della Vita e della Sostenibilità Ambientale, University of Parma, 43124 Parma, Italy

[b]School of Chemistry, Indian Institute of Science Education and Research Thiruvananthapuram (IISER-TVM), Maruthamala PO, Vithura, Thiruvananthapuram - 695551, India

1. Exciton model for a dimer

The monomer has a ground and an excited state, |g> and |e>, respectively, separated by a transition energy ε_M. Both states are non-polar so that the only matrix element of the dipole moment is $\vec{\mu} = \langle g \,|\, \hat{\vec{\mu}} \,|\, e \rangle$

In a dimer composed of two equivalent molecules (A and B in the following) we therefore consider four basis states: $|g_A g_B\rangle$, $|e_A g_B\rangle$, $|g_A e_B\rangle$, $|e_A e_B\rangle$. In the exciton model we only account for the mixing due to electrostatic intermolecular interactions between the two degenerate states $|e_A g_B\rangle$, $|g_A e_B\rangle$. The equivalence of the two molecules leads to very simple expressions for the dimer states, where the two degenerate states are mixed in the symmetric and antisymmetric combinations:

$$|G\rangle = |g_A g_B\rangle$$

$$|E_-\rangle = \frac{1}{\sqrt{2}}\left(|e_A g_B\rangle - |g_A e_B\rangle\right)$$

$$|E_+\rangle = \frac{1}{\sqrt{2}}\left(|e_A g_B\rangle + |g_A e_B\rangle\right)$$

$$|E_E\rangle = |e_A e_B\rangle$$

The dipole moment operator for the dimer is the vectorial sum of the two dipole moments:

$$\hat{\vec{\mu}} = \hat{\vec{\mu}}_A + \hat{\vec{\mu}}_B$$

Accordingly, the transition dipole moment in the dimer can be written as the vectorial sum of the transition dipole moments associated with the two dyes:

$$\langle G \,|\, \hat{\vec{\mu}} \,|\, E_- \rangle = \langle G \,|\, \hat{\vec{\mu}}_A \,|\, E_- \rangle + \langle G \,|\, \hat{\vec{\mu}}_B \,|\, E_- \rangle$$

$$\langle G \,|\, \hat{\vec{\mu}} \,|\, E_+ \rangle = \langle G \,|\, \hat{\vec{\mu}}_A \,|\, E_+ \rangle + \langle G \,|\, \hat{\vec{\mu}}_B \,|\, E_+ \rangle$$

$$\langle G \,|\, \hat{\vec{\mu}} \,|\, E_E \rangle = \langle G \,|\, \hat{\vec{\mu}}_A \,|\, E_E \rangle + \langle G \,|\, \hat{\vec{\mu}}_B \,|\, E_E \rangle$$

The orthogonality of the |g> and |e> states in each molecule, guarantees for a vanishing $\langle G | \hat{\vec{\mu}} | E_E \rangle$ transition dipole moment. The other components of the transition dipole moments read:

$$\vec{\mu}_{-,A} = \langle G | \hat{\vec{\mu}}_A | E_- \rangle = \frac{1}{\sqrt{2}} \vec{\mu}_A$$

$$\vec{\mu}_{-,B} = \langle G | \hat{\vec{\mu}}_B | E_- \rangle = - \frac{1}{\sqrt{2}} \vec{\mu}_B$$

$$\vec{\mu}_{+,A} = \langle G | \hat{\vec{\mu}}_A | E_+ \rangle = \frac{1}{\sqrt{2}} \vec{\mu}_A$$

$$\vec{\mu}_{+,B} = \langle G | \hat{\vec{\mu}}_B | E_+ \rangle = \frac{1}{\sqrt{2}} \vec{\mu}_B$$

Where $\vec{\mu}_A = \langle g_A | \hat{\vec{\mu}}_A | e_A \rangle$ and $\vec{\mu}_B = \langle g_B | \hat{\vec{\mu}}_B | e_B \rangle$

We can now calculate rotational strengths associated to the different transition [1]:

$$R_i = - \frac{\omega_i}{2} \vec{r} \cdot \left(\vec{\mu}_{i,A} \times \vec{\mu}_{i,B} \right)$$

Where i counts on the two excitonic states, i=-,+, and ω_i is the corresponding transition frequency

More in detail:

$$R_- = + \frac{\omega_-}{4} \vec{r} \cdot \left(\vec{\mu}_A \times \vec{\mu}_B \right)$$

$$R_+ = - \frac{\omega_+}{4} \vec{r} \cdot \left(\vec{\mu}_A \times \vec{\mu}_B \right)$$

2. Ultra-exciton model for a dimer

The above equations immediately bring out a fundamental problem of the exciton model which is that it does not obey the sum rule on the rotational strength. Indeed, R_+ and R_- above do not sum to zero because of the different values of ω_+ and ω_-, i.e. precisely because of the exciton splitting.

The complete Hamiltonian for the dimer, written on the basis of the four states, $|g_A g_B\rangle$, $|e_A g_B\rangle$, $|g_A e_B\rangle$, $|e_A e_B\rangle$, reads:

$$H = \begin{pmatrix} 0 & 0 & 0 & V \\ 0 & \varepsilon_M & V & 0 \\ 0 & V & \varepsilon_M & 0 \\ V & 0 & 0 & 2\varepsilon_M \end{pmatrix}$$

where V is the intermolecular interaction energy and ε_M the monomer excitation energy. It is easy to see that the 4-state problem factorizes into two bidimensional problems, one relevant to the two degenerate states, $|e_A g_B\rangle$, $|g_A e_B\rangle$, whose diagonalization leads to the $|E_-\rangle$ and $|E_+\rangle$ discussed above. The diagonalization of the matrix relevant to the $|g_A g_B\rangle$, $|e_A e_B\rangle$ states is trivial so that we get the four dimer states:

$$|G\rangle = \sqrt{1-\rho}\,|g_A g_B\rangle - \sqrt{\rho}\,|e_A e_B\rangle$$

$$|E_-\rangle = \frac{1}{\sqrt{2}}\big(|e_A g_B\rangle - |g_A e_B\rangle\big)$$

$$|E_+\rangle = \frac{1}{\sqrt{2}}\big(|e_A g_B\rangle + |g_A e_B\rangle\big)$$

$$|E_E\rangle = \sqrt{\rho}\,|g_A g_B\rangle + \sqrt{1-\rho}\,|e_A e_B\rangle$$

where

$$\rho = \frac{1}{2}\left(1 - \frac{\varepsilon_M}{\sqrt{V^2 + {\varepsilon_M}^2}}\right) \quad \text{or} \quad \varepsilon_M = \frac{V\ \ 1-2\rho}{2\sqrt{\rho(1-\rho)}}$$

The energies of the four states are:

$$E_G = 2\rho\varepsilon_M - 2V\sqrt{\rho(1-\rho)} = -V\frac{\sqrt{\rho}}{\sqrt{1-\rho}}$$

$$E_{E-} = \varepsilon_M - V$$

$$E_{E+} = \varepsilon_M + V$$

$$E_{EE} = 2(1-\rho)\varepsilon_M + 2V\sqrt{\rho(1-\rho)}$$

The transition dipole moments from the ground to the excited states can be decomposed again in the contributions from molecule A and B

$$\vec{\mu}_{-,A} = \left\langle G \middle| \overleftrightarrow{\mu}_A \middle| E_- \right\rangle = \frac{1}{\sqrt{2}}(\sqrt{1-\rho} + \sqrt{\rho})\vec{\mu}_A$$

$$\vec{\mu}_{-,B} = \left\langle G \middle| \overleftrightarrow{\mu}_B \middle| E_- \right\rangle = -\frac{1}{\sqrt{2}}(\sqrt{1-\rho} + \sqrt{\rho})\vec{\mu}_B$$

$$\vec{\mu}_{+,A} = \left\langle G \middle| \overleftrightarrow{\mu}_A \middle| E_+ \right\rangle = \frac{1}{\sqrt{2}}(\sqrt{1-\rho} - \sqrt{\rho})\vec{\mu}_A$$

$$\vec{\mu}_{+,B} = \left\langle G \middle| \overleftrightarrow{\mu}_B \middle| E_+ \right\rangle = \frac{1}{\sqrt{2}}(\sqrt{1-\rho} - \sqrt{\rho})\vec{\mu}_B$$

$$\vec{\mu}_{E_E,A} = \left\langle G \middle| \overleftrightarrow{\mu}_A \middle| E_E \right\rangle = 0$$

$$\vec{\mu}_{EE,B} = \left\langle G \middle| \overleftrightarrow{\mu}_B \middle| E_E \right\rangle = 0$$

where $\vec{\mu}_A = \left\langle g_A \middle| \overleftrightarrow{\mu}_A \middle| e_A \right\rangle$ and $\vec{\mu}_B = \left\langle g_B \middle| \overleftrightarrow{\mu}_B \middle| e_B \right\rangle$

The rotational strength towards E_E state vanishes, while the rotational strengths to E_- and E_+ are:

$$R_- = -\frac{E_{E_-} - E_G}{2\hbar}\vec{r} \cdot \left(\vec{\mu}_{-,A} \times \vec{\mu}_{-,B}\right) = \frac{E_{E_-} - E_G}{2\hbar}\frac{1}{2}(\sqrt{1-\rho} + \sqrt{\rho})^2\vec{r} \cdot \left(\vec{\mu}_A \times \vec{\mu}_B\right)$$

$$R_+ = -\frac{E_{E_+} - E_G}{2\hbar}\vec{r} \cdot \left(\vec{\mu}_{+,A} \times \vec{\mu}_{+,B}\right) = -\frac{E_{E_+} - E_G}{2\hbar}\frac{1}{2}(\sqrt{1-\rho} - \sqrt{\rho})^2\vec{r} \cdot \left(\vec{\mu}_A \times \vec{\mu}_B\right)$$

Summing up

$$\begin{aligned} R_- + R_+ &= \frac{1}{4\hbar}\left\{\left(\varepsilon_M + V\frac{\sqrt{\rho}}{\sqrt{1-\rho}}\right)4\sqrt{\rho(1-\rho)} - 2V\right\} = \frac{1}{4\hbar}\left\{\left(\frac{V}{2}\frac{1-2\rho}{\sqrt{\rho(1-\rho)}} + V\frac{\sqrt{\rho}}{\sqrt{1-\rho}}\right.\right. \\ &= 0 \end{aligned}$$

3. TD-DFT calculations and exciton model for a chiral dimer

Fig. S1 and S2 shows TD-DFT and exciton model (EM) calculations for a left-handed dimer in helical and creeper geometry. For exciton model calculations, detailed computational results are listed in table S1 (the corresponding table for TD-DFT calculations is in the main text). Here the tilt angle between the interacting dipoles (θ) is varied from 10° to 80° (10° to 40° in fig S1; 50° to 80° in fig S2) with an increment of 10°.

Table S1 *Calculated the oscillator strength (f) and rotational strength (R) of the electronic transitions possible in a dimer at various twist angles (10° - 80°) in helical and creeper geometry using exciton model.*

Right-handed helix: Dimer						
Angle	**Helical**			**Creeper**		
	Trans. energy eV	f	R (× 10^{-54}) $C^2m^3s^{-1}$	Trans. energy eV	f	R (× 10^{-54}) $C^2m^3s^{-1}$
10°	3.93	0.03	366.65	3.94	3.79	-183.68
	3.99	3.83	-372.55	3.98	0.03	185.92
20°	3.93	0.12	722.43	3.94	3.7	-361.88
	3.99	3.75	-733.50	3.98	0.12	366.09
30°	3.93	0.26	1056.75	3.94	3.56	-529.27
	3.99	3.61	-1071.68	3.98	0.26	534.95
40°	3.94	0.45	1359.64	3.94	3.37	-680.84
	3.99	3.41	-1376.61	3.98	0.45	687.29
50°	3.94	0.68	1621.98	3.94	3.13	-812.01
	3.98	3.17	-1638.96	3.98	0.69	818.46
60°	3.94	0.96	1835.81	3.95	2.87	-918.80
	3.98	2.89	-1850.74	3.97	0.96	924.47

70°	3.95	1.26	1994.53	3.95	2.57	-997.93
	3.97	2.58	-2005.61	3.97	1.26	1002.14
80°	3.95	1.58	2093.14	3.96	2.25	-1046.92
	3.97	2.25	-2099.04	3.96	1.59	1049.17

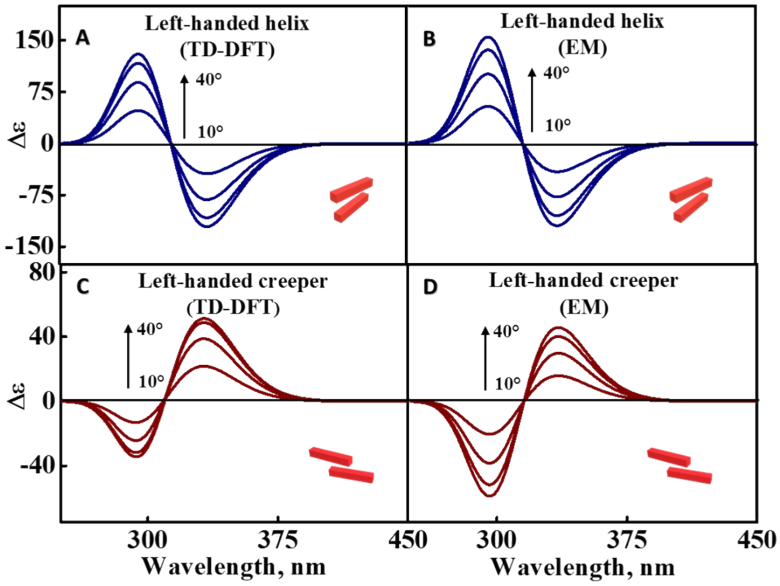

Figure S1 *Computed the CD spectra of a left-handed dimer at different tilt angle (10° - 40°) in helical geometry (A,B) where the interactions are repulsive and in creeper geometry (C,D) where the interactions are attractive using TD-DFT (A,C) and exciton model (B,D) calculations.*

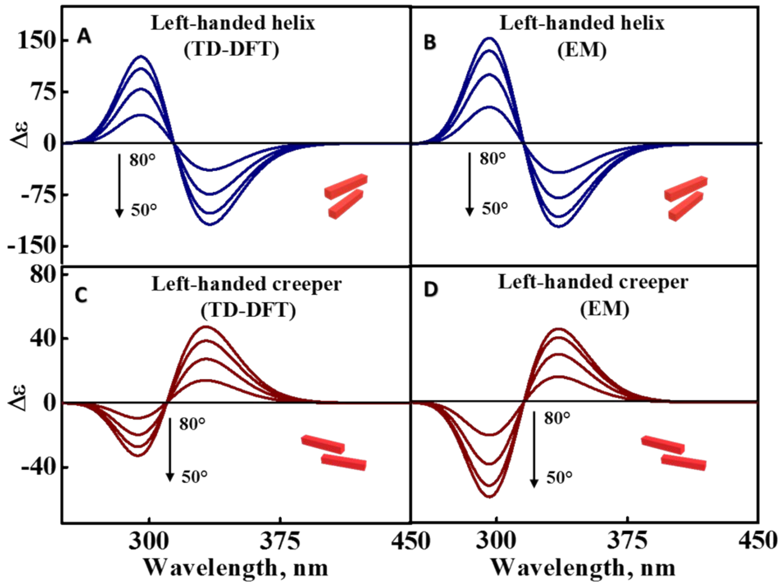

Figure S2 *Computed the CD spectra of a left-handed dimer at different tilt angle (50° - 80°) in helical geometry (A,B) where the interactions are repulsive and in creeper geometry (C,D) where the interactions are attractive using TD-DFT (A,C) and exciton model (B,D) calculations.*

TD-DFT calculations and exciton model for a chiral trimer

For all the TD-DFT calculations, Gaussian 16 suite is used choosing the functional as CAM-B3LYP and basis as 6-31G(d).[2]

Fig. S3 shows the geometrical arrangement of molecules in the trimer and the tilt angle between the adjacent transition dipole moments are denoted. Results are summarized in table S2 (TD-DFT calculations) and table S3 (Exciton model). Calculated CD spectra for right-handed helices and creepers are shown in Fig S4. As observed for the dimer, the exciton method holds for the helix geometry, while it fails for the creeper geometry.

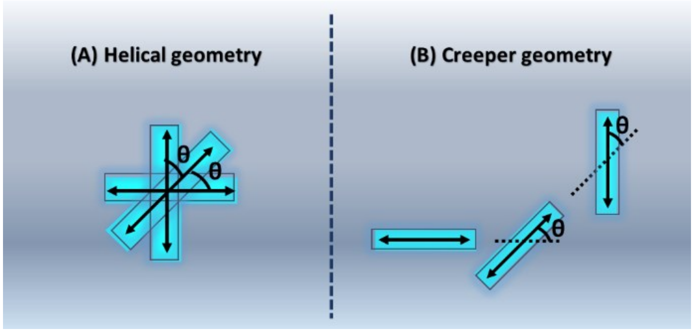

Figure S3 *The tilt angle (θ) between the interacting dipoles are defined in the helical (A) and creeper (B) trimeric assembly in a two-dimensional arrangement. The intermolecular distance between molecules along z is 10 Å for the helix and 5 Å for the creeper.*

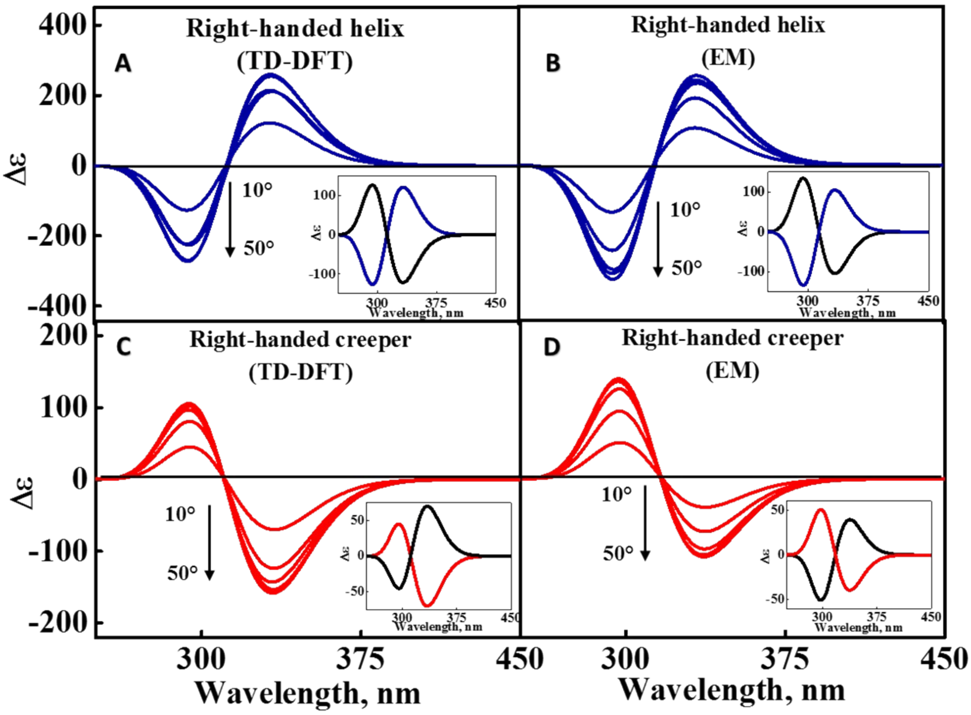

Figure S4 *Calculated the CD spectra of right-handed helical (A,B) and creeper (C,D) trimer at* θ *(10° - 50°) using TD-DFT (A,C) and exciton model (B,D) calculations. For simplicity, only the CD spectra from right-handed arrangement is provided but in the inset of all the graphs the CD spectra for a trimer at a tilt angle of 10° in the right-handed fashion (blue trace for helix and red trace for creeper) and left-handed fashion (black trace) is presented.*

Table S2 *Calculated the oscillator strength (f) and rotational strength (R) of the electronic transitions for a trimeric aggregate at various θ (10° - 50°) in helical and creeper-helical geometry using TD-DFT.*

Right-handed helix: Trimer						
Angle	Helical			Creeper		
	Trans. Energy (eV)	f	R (× 10^{-54}) $C^2m^3s^{-1}$	Trans. Energy (eV)	f	R (× 10^{-54}) $C^2m^3s^{-1}$
10°	3.914	0.088	-148.24	3.91	5.67	-639.60
	3.950	0.11	1392.33	3.96	0.11	689.26
	4.003	5.23	-1234.06	3.98	0.11	-81.52
20°	3.916	0.062	-246.11	3.92	5.35	-1224.22
	3.951	0.43	2616.85	3.96	0.44	1297.75
	4.00	4.95	-2353.07	3.98	0.07	-128.98
30°	3.920	0.029	-248.75	3.92	4.86	-1705.35
	3.953	0.92	3525.52	3.96	0.94	1753.67
	3.995	4.50	-3256.91	3.98	0.03	-115.38
40°	3.924	0.004	-121.6061	3.93	4.23	-2045.70
	3.955	1.52	4008.46	3.96	1.55	1999.20
	3.989	3.94	-3869.72	3.97	0.00	-22.18
50°	3.929	0.005	153.88	3.93	3.52	-2223.06
	3.957	2.16	4007.79	3.96	2.21	2002.72
	3.982	3.31	-4150.20	3.97	0.02	159.51

Table S3 *Computed the oscillator strength (f) and rotational strength (R) of possible electronic transitions in a trimer at various* θ *(10° - 50°) in helical and creeper-helical geometry using exciton model.*

Right-handed helix: Trimer						
Angle	Helical			Creeper		
	Trans. Energy (eV)	f	R $(\times 10^{-54})$ $C^2m^3s^{-1}$	Trans. Energy (eV)	f	R $(\times 10^{-54})$ $C^2m^3s^{-1}$
10 °	3.92	0.11	-173.17	3.92	5.476	-635.39
	3.96	0.12	1454.54	3.96	0.116	728.516
	4.01	5.59	-1295.93	3.99	0.112	-87.54
20 °	3.92	0.08	-287.03	3.93	5.185	-1217.96
	3.96	0.45	2734.13	3.96	0.449	1369.11
	4	5.28	-2473.51	3.99	0.074	-140.76
30 °	3.92	0.04	-288.9	3.93	4.726	-1700.39
	3.96	0.96	3684.68	3.96	0.959	1844.49
	4	4.80	-3429.37	3.99	0.03	-130.30
40 °	3.93	0.01	-139.15	3.93	4.137	-2045.81
	3.96	1.58	4191.45	3.96	1.585	2097.31
	4	4.20	-4087.72	3.99	0.001	-36.15
50 °	3.93	0.01	46.61	3.94	3.465	-2231.51
	3.96	2.25	1058.63	3.96	2.251	2097.09
	3.99	3.52	-1105.24	3.98	0.017	149.33

4. Exciton model for larger aggregates

Fig. S5 reports the calculated CD spectra for an aggregate composed by ten monomers with a twist angle of 45° and 80°. The calculations are performed adopting the exciton model (the system is very large for TD-DFT calculation). Similar to the dimers and trimers, the exciton chirality rule holds only for helices, whereas it collapses in creeper geometry due to the presence of attractive interactions indicating that the rule cannot be adopted for all types of chiral supramolecular structures. It is also important to note that the intensity of the CD spectrum from the aggregate decreases when θ is increased from 45° to 80°.

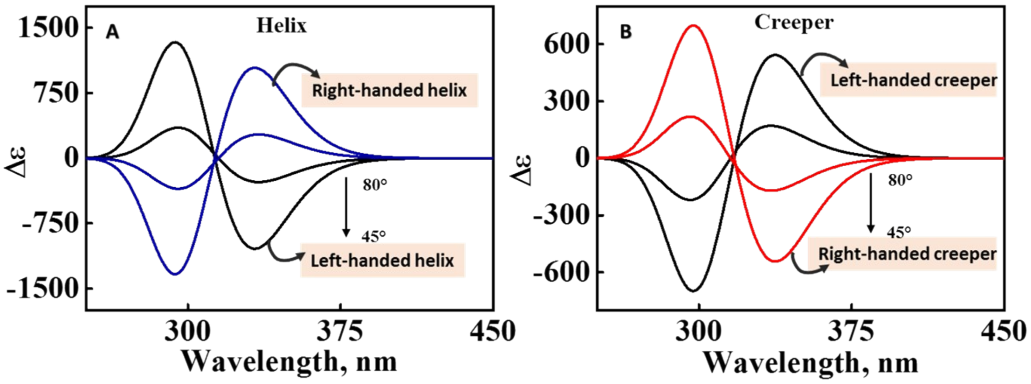

Figure S5 *Estimated the CD spectra of a chiral aggregate in helical (A) and creeper (B) geometry arranged in right-handed (blue trace for helical and red trace for creeper) and left-handed (black trace) fashion with a tilt angle of 45° and 80°.*

6. References

1. D. P. Craig and T. Thirunamachandran, Molecular quantum electrodynamics: an introduction to radiation-molecule interactions, Courier Corporation, 1998.

2. M. J. Frisch, G. W. Trucks, H. B. Schlegel, G. E. Scuseria, M. A. Robb, J. R. Cheeseman, G. Scalmani, V. Barone, G. A. Petersson, H. Nakatsuji, X. Li, M. Caricato, A. V. Marenich, J. Bloino, B. G. Janesko, R. Gomperts, B. Mennucci, H. P. Hratchian, J. V. Ortiz, A. F. Izmaylov, J. L. Sonnenberg, Williams, F. Ding, F. Lipparini, F. Egidi, J. Goings, B. Peng, A. Petrone, T. Henderson, D. Ranasinghe, V. G. Zakrzewski, J. Gao, N. Rega, G. Zheng, W. Liang, M. Hada, M. Ehara, K. Toyota, R. Fukuda, J. Hasegawa, M. Ishida, T. Nakajima, Y. Honda, O. Kitao, H. Nakai, T. Vreven, K. Throssell, J. A. Montgomery Jr., J. E. Peralta, F. Ogliaro, M. J. Bearpark, J. J. Heyd, E. N. Brothers, K. N. Kudin, V. N. Staroverov, T. A. Keith, R. Kobayashi, J. Normand, K. Raghavachari, A. P. Rendell, J. C. Burant, S. S. Iyengar, J. Tomasi, M. Cossi, J. M. Millam, M. Klene, C. Adamo, R. Cammi, J. W. Ochterski, R. L. Martin, K. Morokuma, O. Farkas, J. B. Foresman and D. J. Fox, Journal, 2016.